Title
Fatigue fracture of a cemented Omnifit CoCr femoral stem: implant and failure analysis.

Journal
Arthroplasty today, 3(4)

ISSN
2352-3441

Authors
Bonnheim, Noah
Gramling, Hannah
Ries, Michael
et al.

Publication Date
2017-12-01

DOI
10.1016/j.artd.2017.06.005

Peer reviewed

Arthroplasty Today 3 (2017) 234–238

Contents lists available at ScienceDirect

Arthroplasty Today

journal homepage: http://www.arthroplastytoday.org/

Case report

Fatigue fracture of a cemented Omnifit CoCr femoral stem: implant and failure analysis

Noah Bonnheim, MS [a, *], Hannah Gramling, MS [a], Michael Ries, MD [b], Sanjai Shukla, MD [b], Beatrice Iliescu, MS [c], Lisa Pruitt, PhD [a]

[a] Department of Mechanical Engineering, University of California, Berkeley, CA, USA
[b] Reno Orthopaedic Clinic, Reno, NV, USA
[c] Thayer School of Engineering at Dartmouth College, Hanover, NH, USA

ARTICLE INFO

Article history:
Received 9 January 2017
Received in revised form
7 June 2017
Accepted 10 June 2017
Available online 2 August 2017

Keywords:
Fatigue fracture
Total hip arthroplasty
Stem fracture

ABSTRACT

A cemented, cast CoCr alloy, Omnifit Plus femoral stem was retrieved following mid-stem fracture after 24 years in vivo. The patient was an active 55-year-old male with a high body mass index (31.3) and no traumatic incidents before stem fracture. Fractographic and fatigue-based failure analyses were performed to illuminate the etiology of fracture and retrospectively predict the device lifetime. The fracture surfaces show evidence of a coarse grain microstructure, intergranular fracture, and regions of porosity. The failure analysis suggests that stems with similar metallurgical characteristics, biomechanical environments, and in vivo durations may be abutting their functioning lifetimes, raising the possibility of an increased revision burden.

Introduction

Femoral stem fracture is an established but infrequent complication of total hip arthroplasty. The first generation of Charnley-type, stainless steel femoral stems fractured in approximately 4.1% of patients [1], with fatigue failure attributed to insufficient stem cross-sectional area and inadequate cement support [1,2]. Since the 1970s, improvements in stem design [1] and metallurgy [3] have markedly reduced the incidence of femoral stem fracture. However, reports of femoral stem fracture have continued to surface in the orthopaedic literature, with causes ranging from corrosion at the head-neck interface [4-6] to defects caused by laser etchings [7-9]. Some investigators [10-12] have reported that insufficient proximal bone support may predispose femoral stems to fracture via fatigue loading, while others [13] have suggested that distal fixation is adequate in this system.

A previous report [14] of 9 fractures of cemented, collarless, cast CoCr stems and 1 fracture of a cemented, collared, forged CoCr stem (Omnifit and Omnifit Plus, Osteonics, Allendale, NJ) has linked failure to a coarse metallic grain structure; intergranular corrosion and porosity; and proximal bone loss. Between December 2006 and May 2016, the FDA Manufacturer and User Facility Device Experience database [15] reported at least 13 Omnifit femoral stem fractures occurring at either the neck or mid-stem. Additionally, reports of fractures of forged CoCr femoral stems of various designs, formulations, and manufacturers have also been presented in the literature [7,8,16,17]. Despite improvements in stem design and metallurgy, femoral stem fracture remains a rare but serious complication of total hip arthroplasty.

This case report analyzes the causes of fracture of a cemented, collared, bipolar, cast CoCr alloy, Omnifit Plus femoral stem. We present the results of a stress analysis of the femoral stem based on conditions of both proximal and nonproximal bone support. Furthermore, to elucidate the role of proximal bone support on femoral stem lifetime, we use linear elastic fracture mechanics theory to retrospectively predict the expected device lifetime of the femoral stem for conditions of both proximal and nonproximal bone support.

One or more of the authors of this paper have disclosed potential or pertinent conflicts of interest, which may include receipt of payment, either direct or indirect, institutional support, or association with an entity in the biomedical field which may be perceived to have potential conflict of interest with this work. For full disclosure statements refer to http://dx.doi.org/10.1016/j.artd.2017.06.005.

* Corresponding author. 2121 Etcheverry Hall, Berkeley, CA 94720, USA. Tel.: +1 214 288 1730.
E-mail address: noah.bonnheim@berkeley.edu

http://dx.doi.org/10.1016/j.artd.2017.06.005

Case history

A 55-year-old male patient (height, 72 inches; weight, 230 lb; body mass index, 31.3) had a right hemiarthroplasty in 1990 to treat a femoral neck fracture. The implanted device was a cemented, collared, cast CoCr alloy, Omnifit Plus stem (size #6, 25-mm neck) coupled with a modular, skirted femoral head (26 mm, +10 mm neck extension) and a UHR Universal Head (53 mm). The femoral neck extension was employed presumably to avoid a leg-length discrepancy due to a low femoral neck resection resulting from femoral neck fracture. After 24 years, the patient presented with progressive right hip pain to the point of requiring crutches for ambulation. Physical examination demonstrated weak abduction and flexion muscle activity, and pain associated with straight leg raises, passive flexion, and external and internal rotation. Radiographs (Fig. 1) revealed a mid-stem fracture, acetabular osteolysis, proximal implant migration, and a loose cement mantle. The femoral head appeared to be eccentrically positioned slightly above the center of the outer bipolar component. Additionally, a protrusio acetabular deformity was noted, as was a cortical hypertrophy in the medial mid-femoral diaphysis (Fig. 1).

The patient was scheduled for revision surgery in November of 2014 to remove the failed components and convert the hemiarthroplasty to a total hip arthroplasty. During revision surgery, the distal aspect of the broken stem was found to be well fixed and required an extended trochanteric osteotomy for removal. At the most recent follow-up (approximately 12 months), the patient has shown recovery from the revision surgery, demonstrating acceptable range of motion, return to activities of daily living, and markedly decreased pain.

The implant failure outlined in this article was not reported to the MedWatch program (FDA), as the senior surgical author believed the failure to be an accepted complication of this type of surgery.

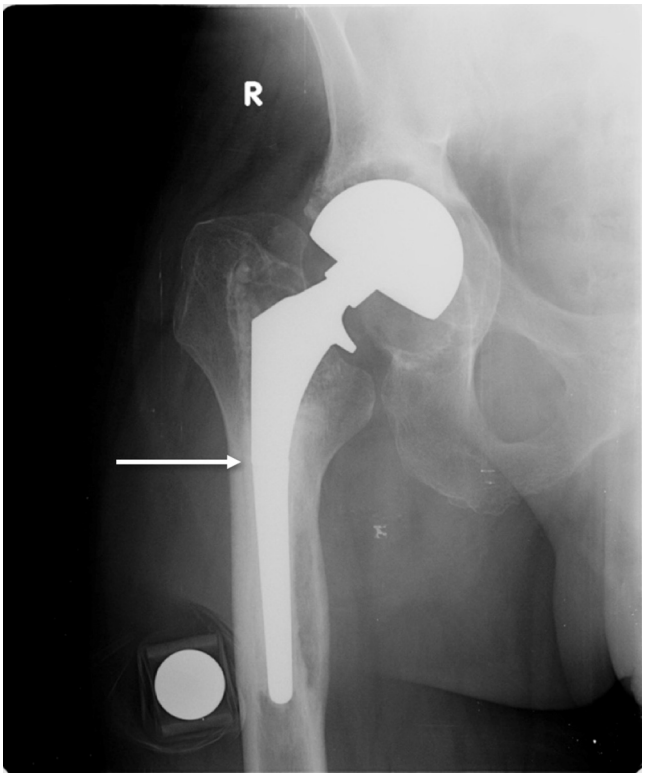

Figure 1. Radiograph of the primary implant reveal a mid-stem fracture, acetabular osteolysis, proximal implant migration, and a loose cement mantle. The location of fracture is denoted by the white arrow.

Fractographic and metallographic analysis

Optical inspection of the implant revealed failure at the midportion of the stem, at approximately 38% of the stem length, measured from the collar (Fig. 2). Low-magnification photographs (Fig. 3) show a large apparent grain structure at the location of fracture.

Fracture surfaces were imaged using a scanning electron microscope (Quanta, FEI, Hillsboro, OR) at the University of California (Berkeley, CA). The fracture surfaces revealed intergranular fracture (Fig. 4a) along with regions of porosity (Fig. 4b) intermittently dispersed on the fracture surface. Observations of fatigue striations are likely masked by martensitic twinning in the alloy structure.

A cross-section immediately distal to the fracture surface was cut and polished using a water-cooled metallurgical diamond saw and progressively finer metallurgical preparation equipment at the Thayer School of Engineering at Dartmouth College (Hanover, NH). Surfaces were etched using a mixture of HCl and HNO_3 (Aqua regia etchant, 3:1 molar ratio) for microstructural characterization. Optical microscopy of the etched surfaces revealed a large dendritic grain structure (Fig. 5a) with generally uniform distribution of carbide precipitates within the grains and a typical accumulation of carbide precipitates at the grain boundaries (Fig. 5b). Grain size (per ASTM E112-13) was measured to be 1.3 ± 0.6 mm (average ± standard deviation).

Stress analysis

Implant stresses at the location of fracture were estimated for 2 conditions: (i) proximal bone support and (ii) fixation exclusively distal to the fracture site (ie, distal fixation). For the case of proximal bone support, an assumption of load sharing between the stem, cement, and bone enabled composite beam theory to be used to estimate stresses at the location of fracture. A 2-dimensional free-body diagram of the leg (Fig. 6a) was used to estimate the angle of joint contact force (θ) and the magnitude of muscle force (F_m). The femoral stem neck dimensions, *a* and *b*, were measured using patient radiographs, and the distance from the greater trochanter to the leg center-of-mass, *c*, was estimated using established anthropometric data [18]. Hip joint contact force has been reported to be approximately 2 times body weight during normal gait [19], and this assumption was used here. As the gluteus medius is thought to provide the largest contribution to peak hip contact force [20], a force reduction assumption was used whereby all

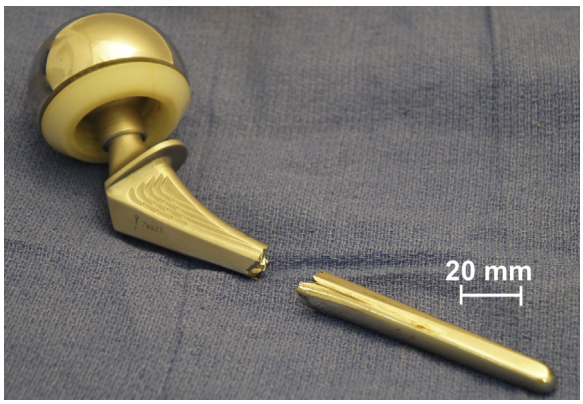

Figure 2. Photograph showing failure at the midportion of the stem, at approximately 38% of the stem length, measured from the collar.

Figure 3. Low-magnification photographs reveal a large apparent grain structure at the location of fracture.

muscle forces other than the gluteus medius were neglected, and muscle force (F_m) was determined using equations for planar static equilibrium. The muscle angle (α) was estimated using patient radiographs, based on the assumption that the gluteus medius insertion point is at the superior-lateral greater trochanter and the pelvic insertion point is at the mid-iliac crest.

The resultant axial and shear forces (R_y and R_x) and moment (M) at the location of fracture were calculated based on the free-body diagram in Fig. 6b. Cross-sectional properties of the bone-cement-implant composite at the site of fracture were estimated using radiographic as well as physical implant measurements. The cortical bone cross-section was modeled as a hollow cylinder with a 33.5-mm outer diameter and a 4.1-mm-thick cortical shell, and the implant cross-section was modeled using physical implant measurements of the stem taken at the location of fracture. Poly(methyl methacrylate) bone cement was assumed to fill the remaining space (Fig. 6c).

Axial and bending stresses in the implant were calculated using classical composite beam theory for 3-material beams in bending. Bending stress is known to be maximum at the fiber farthest from the neutral axis of the composite beam, whereas axial stress (compressive) is assumed constant across the cross-section. Shear stresses were assumed to be small compared with bending stresses and were neglected here. As cyclic tensile loading dominates the fatigue crack propagation in metallic alloys, and the fracture of femoral stems has historically originated on the tensile (lateral) side of the implant, the location of largest tensile stress (ie, lateral implant fiber) was of primary interest in this analysis. The combination of axial and bending stresses at this location yields an estimated stress value of 170 MPa. This number represents the calculated maximum tensile stress experienced by the implant at the location of fracture for the case of full proximal bone support during normal gait.

Radiographic evidence of proximal bone loss and implant loosening raise the possibility of cantilever stem bending behavior resulting from purely distal fixation. This theory is supported by the cortical hypertrophy observed in the mid-femoral diaphysis, which may have been caused by atypical distal load transfer. Thus, a second model (Fig. 7) was used to estimate implant stresses based on the scenario of fixation exclusively distal to the fracture site. Classical beam theory based on planar static equilibrium yielded an estimated maximum tensile stress of 198 MPa.

Fatigue analysis based on linear elastic fracture mechanics was then used to compare life estimates of the femoral stem for the cases of proximal bone support and distal fixation. In this methodology, the number of cycles to failure (N_f) is dictated by the growth of an initial flaw (a_i) to a flaw of critical size for fracture (a_c). Based on the fracture toughness (K_{IC}) for cast CoCr (60 MPa$\sqrt{m}$) [21], the critical flaw size for fracture (Equation 1) was determined by

$$a_c = \left[\frac{K_{IC}}{\gamma \Delta\sigma}\right]^2 \left[\frac{1}{\pi}\right] \tag{1}$$

where γ is a geometric constant (1.12 for the case of an edge-crack tension geometry in which the crack length is sufficiently smaller than the specimen thickness, as described in [22]), and $\Delta\sigma$ is the cyclic stress range (assumed to be 0 to maximum tensile stress for each scenario). Integration of the Paris equation (Equation 2), which relates rate of crack advance to stress intensity range, between the limits of an initial and critical flaw size enables the finite prediction of femoral stem lifetime (Equation 3).

$$\frac{da}{dN} = C\Delta K^m \tag{2}$$

$$N_f = \left[\frac{2}{(m-2)C\gamma^m(\Delta\sigma)^m\pi^{m/2}}\right]\left[\frac{1}{a_i^{(m-2)/2}} - \frac{1}{a_c^{(m-2)/2}}\right] \tag{3}$$

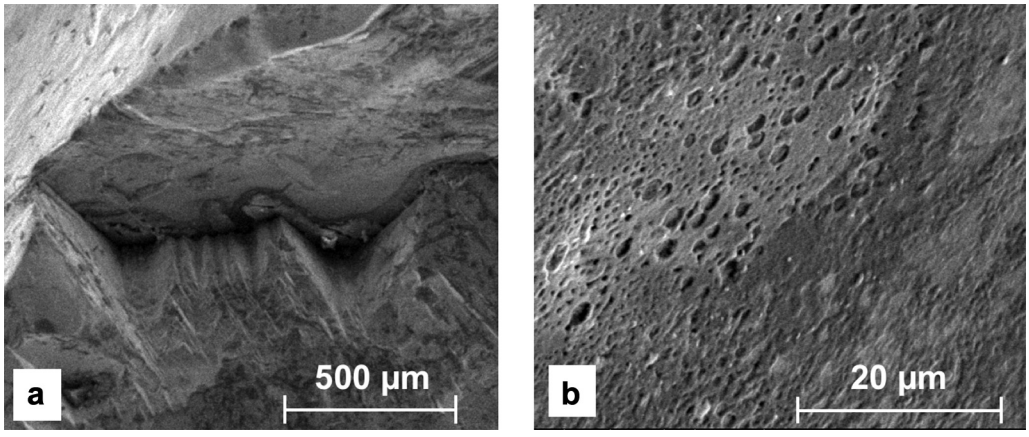

Figure 4. Scanning electron microscopy images of the fracture surface show (a) intergranular fracture (b) regions of porosity.

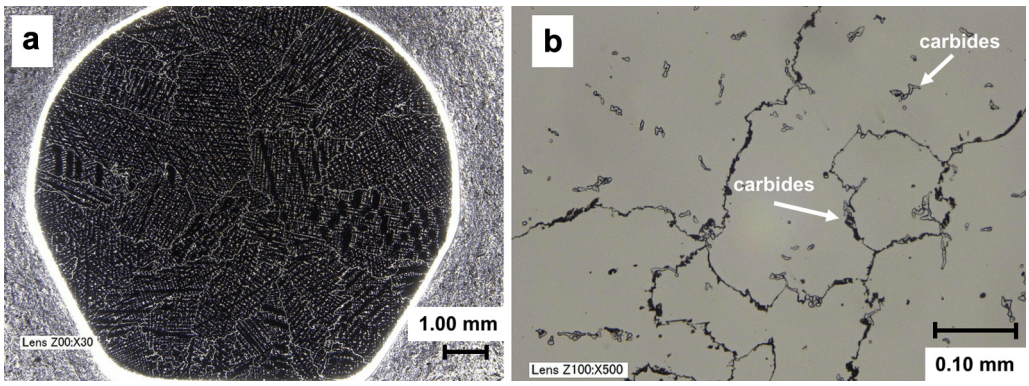

Figure 5. Optical images of the etched surfaces cross-sectioned near the site of fracture showing (a) large dendritic grain structure and (b) uniformly distributed carbide precipitates within the grains and at the grain boundaries.

In Equations 1-3, m is the Paris law exponent and C is fatigue crack propagation constant (for cast CoCr alloys with coarse dendritic grain structures, these values have been reported to be $m = 8.7$ and $C = 4.0 \times 10^{-20}$ m/cycle per MPa$\sqrt{\text{m}^{\text{m}}}$, as described in [23]).

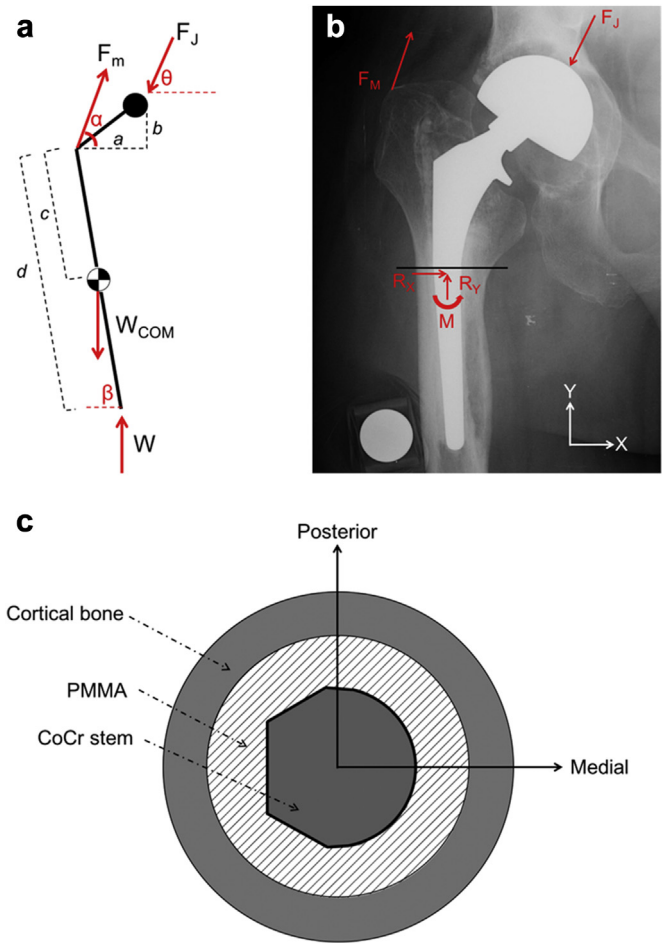

Figure 6. Implant model for the case of proximal bone support showing (a) 2-dimensional free-body diagram of the leg. The dimensions, a and b, were measured using patient radiographs whereas the distance from the greater trochanter to the leg center-of-mass, c, was estimated using established anthropometric data [18]. (b) Free-body diagram used to determine the resultant axial and shear forces, R_y and R_x, and moment (M) at the location of fracture. (c) Cross-sectional properties of the bone-cement-implant composite at the site of fracture, estimated using radiographic as well as physical implant measurements. Poly(methyl methacrylate) bone cement was assumed to fill the space between the implant and cortical bone.

Metallographic analysis revealed an average grain size of 1.3 ± 0.6 mm, and the lower end of this range (0.7 mm) was used as the estimate of initial flaw size, a_i. Based on the conservative assumption of one million steps per year, the expected life of the femoral stem was calculated to be 27.8 years for the case of proximal bone support and 7.3 years for the case of purely distal fixation.

Discussion

Fatigue fracture remains an important failure mechanism in CoCr alloy stems [5,14,15]. The published literature [5,14] describing 14 of 27 Omnifit fractures has implicated deficient metallurgy, as evidenced by a coarse grain microstructure and intergranular fracture, as a driving force of fracture in the forged versions of these designs.

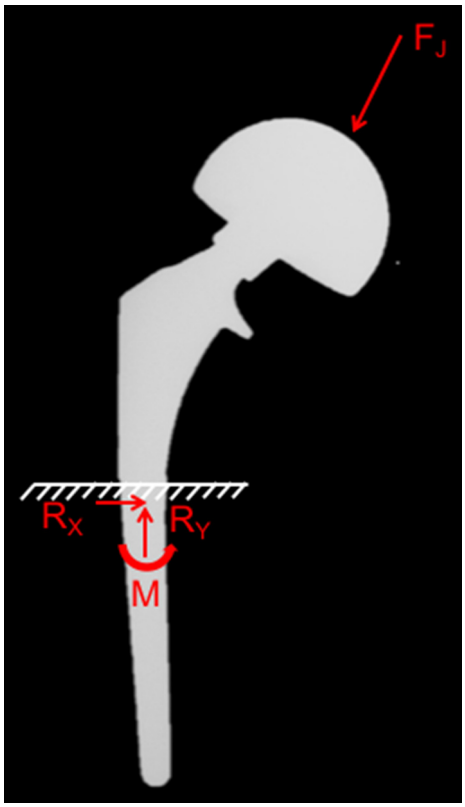

Figure 7. Free-body diagram used to estimate implant stresses at the location of fracture for the case of fixation exclusively distal to the fracture site.

Our fractographic and metallographic analyses of the cast stem similarly reveal a large grain microstructure, intergranular fracture, and regions of porosity. However, while our findings prompt a closer metallurgical analysis to assess the device for metallurgical defects, the etched surfaces did not show evidence of intergranular irregularities. Our stress and failure analyses show that, under the stress conditions of this patient, defects on the order of the grain size of this stem can propagate to failure in approximately 28 years under the optimal condition of full proximal bone support. If proximal bone support is lost, as may occur naturally with age [24] or with osteolytic resorption secondary to polyethylene or other particulate debris [25], the fatigue life may be severely reduced. While improvements in manufacturing and metallurgy may have mitigated the risk of fatigue fracture in more modern stems, the population of historic stems implanted with metallurgical characteristics similar to those presented here may face an increased revision burden as their in vivo duration approaches 30 years.

The observed eccentric positioning of the femoral head within the outer bipolar component indicates the occurrence of wear between the inner ultra-high molecular weight polyethylene bearing and the femoral head, which likely contributed to the noted acetabular osteolysis. This wear-induced eccentric positioning can also be associated with a binding-type loss of motion at the inner bearing, resulting in compensatory motion between the outer CoCr surface and the bony acetabulum. This phenomenon likely contributed to the development of the observed protrusio deformity, which can functionally restrict hip range of motion and thereby cause greater torsional and bending loads on the stem. The possible increase in loading on the stem resulting from this alteration in normal joint kinematics may also have contributed to the failure presented here.

Summary

This case study illustrates that fatigue failure of CoCr stems remains a long-term failure mechanism when used in biomechanically demanding in vivo environments. When proximal bone loss occurs, the cyclic stresses experienced within the shaft of the stem can increase, thereby reducing the cycles to fracture. The hypothesized mechanism of fracture in the presented case is that large grains and pores served as fracture initiation sites, which then propagated through the stem until fracture. Fracture of stems with similar metallurgy and in vivo loading conditions may continue to occur as their time in vivo increases.

Acknowledgments

The authors would like to thank Professor Douglas W. Van Citters for helpful discussions regarding interpretations of the metallographs.

References

[1] Dall D, Learmonth I, Solomon M, et al. Fracture and loosening of Charnley femoral stems. J Bone Joint Surg Br 1993;75-B(2):259.
[2] Charnley J. Fracture of femoral prostheses in total hip replacement. Clin Orthop Relat Res 1975;111:105.
[3] Sudhakar K, Wang J. Fatigue behavior of Vitallium-2000 Plus alloy for orthopedic applications. J Mater Eng Perform 2011;20(6):1023.
[4] Gilbert J, Buckley C, Jacobs J, et al. Intergranular corrosion-fatigue failure of cobalt-alloy femoral stems. J Bone Jt Surg 1994;76-A(1):110.
[5] Lam L, Stoffel K, Kop A, et al. Catastrophic failure of 4 cobalt-alloy Omnifit hip arthroplasty femoral components. Acta Orthop 2008;79(1):18.
[6] Hamlin K, MacEachern C. Fracture of an exeter stem. J Bone Jt Surg Case Connect 2014;4(5).
[7] Lee E, Kim H. Early fatigue failures of cemented, forged, cobalt-chromium femoral stems at the neck-shoulder junction. J Arthroplasty 2001;16(2):236.
[8] Woolson S, Milbauer J, Bobyn J, et al. Fatigue fracture of a forged cobalt-chromium-molybdenum femoral component inserted with cement. A report of ten cases. J Bone Jt Surg 1997;79-A(12):1842.
[9] Buttaro M, Mayor M, Van Citters D, et al. Fatigue fracture of a proximally modular, distally tapered fluted implant with diaphyseal fixation. J Arthroplasty 2007;22(5):780.
[10] Crowninshield R, Maloney W, Wentz D, et al. The role of proximal femoral support in stress development within hip prostheses. Clin Orthop Relat Res 2004;420:176.
[11] Andriacchi T, Galante J, Belytschko T, et al. A stress analysis of the femoral stem in total hip prostheses. J Bone Jt Surg 1976;58-A(5):618.
[12] Busch C, Charles M, Haydon C, et al. Fractures of distally-fixed femoral stems after revision arthroplasty. J Bone Jt Surg 2005;87-B(10):1333.
[13] Murphy S, Rodriguez J. Revision total hip arthroplasty with proximal bone loss. J Arthroplasty 2004;19(4):115.
[14] Della Valle A, Becksac B, Anderson J, et al. Late fatigue fracture of a modern cemented forged cobalt chrome stem for total hip arthroplasty: a report of 10 cases. J Arthroplasty 2005;20(8):1084.
[15] FDA. MAUDE - Manufacturer and User Facility Device experience [Internet]. https://www.accessdata.fda.gov/scripts/cdrh/cfdocs/cfmaude/results.cfm [accessed 08.03.16].
[16] Jazrawi L, Della Valle C, Kummer F, et al. Catastrophic failure of a cemented, collarless, polished, tapered cobalt-chromium femoral stem used with impaction bone-grafting: a report of two cases. J Bone Jt Surg 1999;81-A(6):844.
[17] Miller E, Shastri R, Shih C. Fracture failure of a forged vitallium prosthesis. J Bone Jt Surg 1982;64-A(9):1359.
[18] Bartel D, Davy D, Keaveny T. Orthopaedic Biomechanics: Mechanics and Design in Musculoskeletal Systems. Upper Saddle River, NJ: Pearson Education; 2006. p. 49.
[19] Stansfield B, Nicol A, Paul J, et al. Direct comparison of calculated hip joint contact forces with those measured using instrumented implants. An evaluation of a three-dimensional mathematical model of the lower limb. J Biomech 2003;36:929.
[20] Correa T, Crossley K, Kim H, et al. Contributions of individual muscles to hip joint contact force in normal walking. J Biomech 2010;43:1618.
[21] Pruitt L, Chakravartula A. Mechanics of biomaterials: fundamental principles for implant design. New York, NY: Cambridge University Press; 2011.
[22] Anderson T. Fracture mechanics: fundamentals and applications. 3rd ed. Boca Raton, FL: CRC Press; 2005.
[23] Zhuang L, Langer E. Study on fatigue threshold behaviour and fatigue crack propagation in a cast Co-Cr-Mo alloy used for surgical implants. Fatigue Fract Eng Mater Struct 1989;12(4):283.
[24] Reeve J, Loveridge N. The fragile elderly hip: mechanisms associated with age-related loss of strength and toughness. Bone 2014;61:138.
[25] Maloney W, Smith R. Periprosthetic osteolysis in total hip arthroplasty: the role of particulate wear debris. J Bone Jt Surg 1995;77-A(9):1448.